

Effective Nuclear Charges for the First- through Third-Row Transition Metal Elements in Spin–Orbit Calculations

Shiro Koseki,^{*,†} Michael W. Schmidt,[‡] and Mark S. Gordon^{*,‡}

Chemistry Department for Materials, Faculty of Engineering, Mie University, Tsu 514, Japan, and Department of Chemistry, Iowa State University, Ames, Iowa 50011

Received: August 21, 1998; In Final Form: October 20, 1998

The effective nuclear charges (Z_{eff}), which are empirical parameters in an approximate spin–orbit Hamiltonian, are determined for the first- through third-row transition metal elements by using experimental results for the fine structure splittings in atomic terms. All calculations use multiconfiguration self-consistent-field (MCSCF) wave functions, whose active space includes nd and $(n + 1)sp$ orbitals (n is the principal quantum number), with the effective core potential (ECP) basis sets proposed by Stevens et al., augmented by one set of polarization f functions. First-order or second-order configuration interaction (FOCI or SOCI) calculations were also performed in order to understand disagreements between the MCSCF results and the experimental ones.

1. Introduction

Vibronic and spin–orbit couplings have received much attention in recent theoretical studies.^{1–5} Since such couplings are the major mechanism for electronic transitions between adiabatic potential energy surfaces with the same or different spin states, they frequently play an important role in the estimation of dynamical properties of chemical reactions. Unfortunately, at present, only a few electronic structure codes have the capability to estimate such couplings in general molecular systems.

We have been developing a general code for the estimation of spin–orbit coupling within a one-electron approximation^{6–9}

$$H_{\text{so}} \approx \frac{\alpha^2}{2} \sum_i \sum_A \frac{Z_{\text{eff}}(A)}{r_{iA}^3} L_{iA} S_i$$

in which the neglect of the two-electron terms is compensated for by introducing a semiempirical parameter, the effective nuclear charge (Z_{eff}).^{10–11} α is the fine structure constant, and L and S are orbital and spin angular momentum operators for electron i and nucleus A , respectively. The effective nuclear charges Z_{eff} have previously been determined for the second- through sixth-row main group elements.¹⁰ When effective core potential (ECP) basis sets are employed, these charges do not explain the shielding effect of nuclear charges in the traditional sense, but they are simply empirical parameters to compensate for the neglect of the two-electron part of the spin–orbit interaction and the deficiency of the nodeless ECP orbitals. Our studies provide reliable predictions for spin–orbit splittings in diatomic molecules, with average errors on the order of 10–30%. This approximation has been successfully applied to several small molecular systems.^{10b,11} Therefore, here, we propose effective nuclear charges for the first- through third-row transition metal elements. In subsequent papers, we will

report relativistic potential surfaces of some transition metal hydrides and oxides, as well as polyatomic molecules.

2. Method of Calculation

The SBKJC^{12b,c} ECP basis set is used, augmented with a set of f polarization functions,¹³ in order to be consistent with our previous studies that employed the SBK main group basis sets^{12a} with a set of d polarization functions.^{10b,c} Even though the polarization functions are not important for the determination of the effective nuclear charges in atoms, they will be important for the description of molecular states.

Multiconfiguration self-consistent-field (MCSCF) wave functions¹⁴ are required to describe low-lying degenerate atomic states of transition metals. The active space for these MCSCF calculations includes nd and $(n + 1)sp$ orbitals, where n is the principal quantum number ($n = 3–5$); that is, four semicore orbitals are frozen and nine orbitals are active. The MCSCF orbitals are separately optimized for each state of interest (see the next section) and employed to construct a spin–orbit configuration interaction (CI) matrix. The spin–orbit CI matrix includes the state of interest and its MCSCF virtual states (both same and different spin states); only energetically low-lying electronic states were included in the matrix, and the size of each matrix was restricted to be smaller than 350. The diagonalization of the CI matrix gives the spin–orbit splittings only for the state of interest. This process is repeated using orbitals optimized for each specific desired state of the atom. MCSCF + second-order CI (SOCIO) wave functions were also used for an estimation of the spin–orbit splittings in several electronic states. All calculations reported here were carried out with the quantum chemistry code GAMESS,¹⁵ to which new subroutines were added.

3. Results and Discussion

Spectroscopic data for hydrides have been used to determine the effective nuclear charges (Z_{eff}) for main group elements. Since our main purpose is to estimate spin–orbit coupling in polyatomic molecules, molecular spectroscopic data are ap-

* To whom correspondence should be addressed.

[†] Mie University.

[‡] Iowa State University.

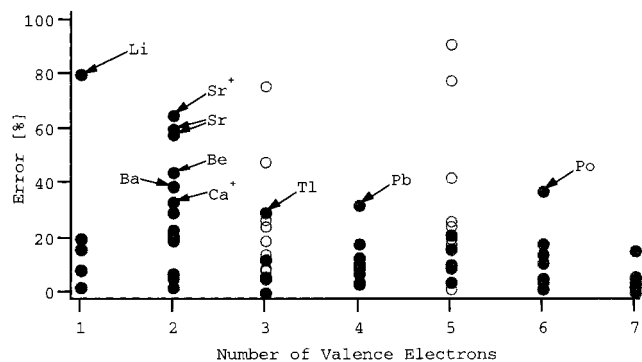


Figure 1. Percentage difference between the calculated energy splittings and the corresponding experimental ones: (●) lowest electronic states whose azimuthal quantum number is nonzero; (○) other electronically excited states.

appropriate for the determination of such empirical parameters.^{10a,b} However, due to the paucity of available spectroscopic data for transition metal hydrides,¹⁶ especially third-row transition metal hydrides, it is impractical to determine Z_{eff} for the transition metal elements based on molecular data. Since there is more atomic spectroscopic data for these elements, these are employed to obtain the empirical parameters.

3.1. Main Group Elements in the Second through Sixth Row. It is useful to examine the reliability of main group Z_{eff} , which have been determined on the basis of hydride spectroscopic data^{10a,b} for the prediction of spin–orbit splittings in atomic states. Figure 1 compares the calculated and experimental energy splittings for 53 low-lying electronic states whose azimuthal quantum number is nonzero, namely, ^2P , ^3P , ^4P , and a few ^2D states (Table 1). Note that S states as well as singlet states, which are generated as low-lying virtual states in MCSCF calculations, were also included in the spin–orbit CI matrixes.

An error of more than 30% is found in Li (^2P), Be (^3P), Ca^+ (^2P), Sr (^3P), Sr^+ (^2P), Pb (^3P), Bi (^2D), and Po (^3P). The splittings, $^3\text{P}_0\text{--}^3\text{P}_1$ and $^3\text{P}_1\text{--}^3\text{P}_2$, are in error by more than 30% in Be and Sr; the error for Tl (^2P) is 29%. In Li (^2P) and Be (^3P), the spin–orbit splittings themselves are quite small (less than 10 cm^{-1}); it appears to be difficult to reproduce such small splittings within the one-electron approximation. Similarly, the spin–orbit splittings of the lowest ^2D and ^2P states in the N atom are smaller than 10 cm^{-1} and are not included in Figure 1.

There is about a 20% error in the calculated splittings for the lowest ^3P state of Ca atom, while there is an error of larger than 30% in the lowest ^2P state of Ca^+ ion. The lowest excited state in Ca^+ ion is ^2D ($4s^13d^1$), and the ^2P state is the second excited state. Therefore, if 3d orbitals are included in the MCSCF active space and the ^2D state is added to the spin–orbit CI matrix, the $^2\text{P}_{3/2}$ substate would strongly interact with $^2\text{D}_{3/2}$ and be energetically lifted by spin–orbit interaction. As a

result, a larger splitting energy would be obtained for the ^2P state. A similar interaction would occur in Sr (^3P) and Sr^+ (^2P), whose lowest P states have small energy splittings with an error of about 60%. As described previously,^{10b} the splittings calculated in sp space can be unreliable for alkaline earth compounds, resulting in predictions of spin–orbit splittings for the alkaline earth elements that are seriously in error. In these elements, low-lying ns^1nd^1 states need to be included in spin–orbit CI matrixes. Unfortunately, the SBK main group basis set is not appropriate and better (larger) ECP basis sets will be required to investigate this problem further.

It is difficult to determine Z_{eff} for the sixth-row elements since there is such a small amount of spectroscopic data for sixth-row atoms and hydrides. We finally have chosen $f_6 = 222$, where $Z_{\text{eff}}(\text{Pb}) = Z(\text{Pb})f_6$ and $Z(\text{Pb})$ is the true nuclear charge of atomic Pb. This is approximately equal to the value reported previously for Pb atom.¹¹ Since Tl has a semicore SBK basis set, $f_6 = 113$ is employed only for Tl atom. Using these f_6 values, we estimated the spin–orbit splittings for Cs (^2P , an error of 20%), Ba (^3P , 21% and 29%), Ba^+ (^2P , 39%), Tl (^2P , 29%), Tl^+ (^3P , 12% and 9%), Pb (^3P , 10 and 32%), Bi (^2D , 16%), and Po (^3P , 18% and 37%). There is no experimental data available for At (^2P).

$Z_{\text{eff}} = 133$ for Tl overestimates the splittings of the lowest atomic ^2P states, but it does reproduce the experimental splittings of the lowest ^3P state in TIH within an error of less than 5%. A relatively large error is found in the lowest P states of Ba and Ba^+ atoms; this result is roughly consistent with the results of Ca and Sr atoms. The predicted $^3\text{P}_0\text{--}^3\text{P}_1$ splitting in atomic Pb is 10% smaller than the corresponding experimental value, while the $^3\text{P}_1\text{--}^3\text{P}_2$ gap is larger than the experimental value by 32%. The same trend is found in the lowest ^3P state of atomic Po. Since Rydberg states, whose main configuration has a 7s electron, appear as the third (Po) and fourth (Pb) lowest states in these elements, it seems that the interaction with the lowest ^5S and/or ^3P Rydberg states strongly stabilizes the $J = 1$ or 2 states of the ^3P valence state.

Disagreement is also found to be somewhat more serious in higher states, since the contribution of Rydberg states is more important for these atomic states and Rydberg orbitals have not been included in the basis set or the active space for these calculations. In general, it appears that (with a few exceptions) spin–orbit splittings of atomic states in main group elements may be predicted within an error of 10–30% if the basis set and the MCSCF active space are large enough to reasonably describe the electronic states of interest. For example, the error in the $^3\text{P}_1\text{--}^3\text{P}_2$ splitting for the lowest ^3P state in Pb atom is reduced from 32% to 25% when the external sp orbitals are included in the MCSCF active space.

Thus, although the average error in the calculated splittings is somewhat larger than those in diatomic molecules,^{10b} 66%

TABLE 1: Electronic States of Main Group Elements^a

	2	3	4	5	6
1	Li (^2P)	Na (^2P)	K (^2P)	Rb (^2P)	Cs (^2P)
2	Be (^3P)	Mg (^3P), Mg^+ (^2P)	Ca (^3P), Ca^+ (^2P)	Sr (^3P), Sr^+ (^2P)	Ba (^3P), Ba^+ (^2P)
3	B (^2P , ^4P)	Al (^2P , ^4P)	Ga (^2P , ^4P)	In (^2P , ^4P)	Tl (^2P , ^4P)
4	C (^3P)	Si (^3P)	Ge (^3P)	Sn (^3P)	Pb (^3P)
5	N (^2D , ^2P , ^4P) N^+ (^3P)	P (^2D , ^2P , ^4P)	As (^2D , ^2P , ^4P)	Sb (^2D , ^2P)	Bi (^2D , ^2P)
6	O (^3P) O^{2+} (^3P)	S (^3P)	Se (^3P)	Te (^3P)	Po (^3P)
7	F, F^{2+} (^2P) F^+ , F^{3+} (^3P)	Cl (^2P)	Br (^2P)	I (^2P)	At (^2P)

^a Row shows the number of valence electrons and the column shows the row number in the periodic table of main group elements.

TABLE 2: Electronic States of Transition Metal Elements^a

	1	2	3
3	Sc (² D, ² F, ⁴ F), Sc ²⁺ (² D, ² S, ² P)	Y (² D, ² P, ⁴ F, ⁴ F)	La (² D, ² F, ⁴ F, ⁴ P)
4	Ti (³ F, ³ P, ⁵ F), Ti ²⁺ (³ F, ³ P)	Zr (³ F, ³ P, ⁵ F)	Hf (³ F, ³ P, ⁵ F)
5	V (⁴ F, ⁶ D), V ²⁺ (² P, ² G, ⁴ F, ⁴ P)	Nb (² G, ² D, ⁴ F, ⁴ P, ⁴ D, ⁶ D)	Ta (² G, ⁴ F, ⁴ P, ⁶ D)
6	Cr (³ P, ⁵ D, ⁵ G, ⁵ P), Cr ²⁺ (³ P, ³ H, ⁵ D)	Mo (⁵ D, ⁵ G)	W (³ P, ³ H, ⁵ D)
7	Mn (⁶ D, ⁸ P)	Tc (⁴ D, ⁴ P, ⁴ F, ⁶ D)	Re (⁴ P, ⁴ G, ⁴ D, ⁶ D)
8	Fe (³ F, ³ P, ⁵ D, ⁵ F, ⁵ P), Fe ²⁺ (³ P, ³ H, ⁵ D)	Ru (³ F, ⁵ F, ⁵ D, ⁵ P)	Os (³ F, ⁵ D, ⁵ F)
9	Co (² F, ⁴ F, ⁴ F), Co ²⁺ (² G, ² H, ⁴ F, ⁴ P)	Rh (² D, ² F, ² P, ⁴ F, ⁶ P)	Ir (² P, ² F, ² G, ⁴ F, ⁴ P)
10	Ni (³ F, ³ D, ³ P, ⁵ D), Ni ²⁺ (³ F, ³ P, ⁵ F)	Pd (³ D, ³ F, ³ P)	Pt (³ D)
11	Cu (² D, ² P, ⁴ P), Cu ²⁺ (² D, ² F, ⁴ F)	Ag (² P, ² D)	Au (² D, ² P)
12	Zn (³ P)	Cd (³ P)	Hg (³ P)

^a Each row gives the number of nd , $(n + 1)s$, and $(n + 1)p$ electrons, where n is the principal quantum number; each column labels the row number (first, second, or third) in the periodic table of transition metal elements.

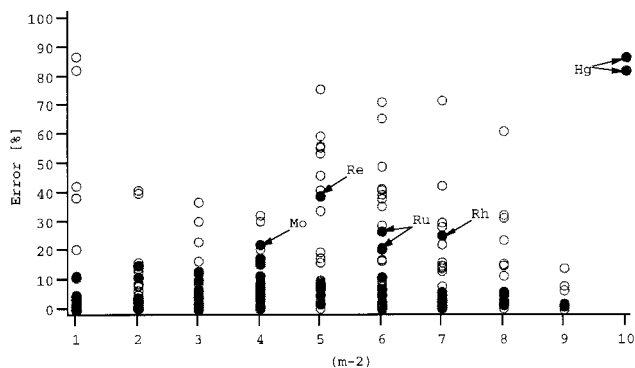


Figure 2. Percentage difference between the calculated energy splittings and the corresponding experimental ones. m , on the abscissa, is the number of MCSCF active electrons: (●) lowest electronic states whose azimuthal quantum number is nonzero; (○) other electronically excited states. The error is larger than 100% in Zn and Cd.

of the energy splittings are predicted to be within 20% of the experimental values, and 83% of the calculated values are within 40% of the experimental values.

3.2. Determination of Z_{eff} for the Transition Metals. Moore's spectroscopic data¹⁷ have been used to determine the effective nuclear charges Z_{eff} for transition metal elements.

$$Z_{\text{eff}}(A) = Z(A)f_k$$

$$f_1 = 0.385 + 0.025(m - 2) \text{ (first-row)}$$

$$f_2 = 4.680 + 0.060(m - 2) \text{ (second-row)}$$

$$f_3 = 13.960 + 0.140(m - 2) \text{ (third-row)}$$

where $Z(A)$ is the nuclear charge of atom A and m is the number of nd and $(n + 1)sp$ electrons. As discussed in the previous paper,^{10b} SBKJC 3d orbitals are qualitatively similar to correct 3d atomic orbitals, whereas 4d and 5d SBKJC orbitals are nodeless. As a result, Z_{eff} is smaller than the actual nuclear charge for the first-row transition elements ($f_1 < 1$), but the lack of the correct radial nodes means that relatively large Z_{eff} for the heavier elements are needed to reproduce the experimental atomic splittings.¹⁸

Using these values for Z_{eff} , the spin-orbit splittings are predicted for 98 low-lying atomic electronic states whose electron configurations are $(nd)^a(n + 1)s^b(n + 1)p^c$ (a , b , and c are occupation numbers), in the first- through third-row transition metal elements (Table 2). The errors in the calculated splittings are plotted in Figure 2, where 48 states are for the first row, 26 are for the second row, and 24 are for the third row. Unfortunately, the MCSCF calculation gives us an incorrect energetic order of atomic terms in Os, Ir, and Pt so that their

results are excluded from Figure 2. We will discuss these in the following paragraphs.

The Z_{eff} method appears to be reasonable for low-lying electronic states, except for Zn, Cd, and Hg ($m - 2 = 10$; the error is larger than 100% in Zn and Cd), since the error in calculated splittings is generally less than 20% in the lowest states whose azimuthal quantum number is nonzero. The trend for excited electronic states is similar to that noted above for main group elements. As a whole, 70% of the energy splittings are predicted to be within 20% of the experimental values, and 81% of the calculated values are within 40% of the experimental values. In the remaining paragraphs of this section, we comment only on the cases where the results are appreciably in error.

The Z_{eff} values for Fe, Mo, and Pt have been determined independently.¹⁹ The Fe Z_{eff} of 14.1 found by Heinemann et al.¹⁹ is close to our value (13.91). Solomonik²⁰ reported 213 for the Mo atom, compared with 206.64 in the present work. Schmidt's value for Pt (916.5, $f_3 = 11.75$)²¹ is smaller than our value (1176.24, $f_3 = 15.08$). Heinemann et al. also have examined the splittings of Pt atom using several Z_{eff} values.²² They concluded, "a scaling parameter Z_{eff} between 950 and 1200 reproduces more rigorous treatments of spin-orbit effects on spectroscopic constants and low-lying excited-state energies in platinum-containing species in a semiquantitative manner".

Our MCSCF splittings in Pt atom are not in good agreement with the experimental ones (not shown in Figure 2); the $^3D_2 - ^3D_1$ splitting is almost equal to the experimental value, but an error of 114% is found for the $^3D_3 - ^3D_2$ splitting. This may be due to the inability of the MCSCF calculations to correctly predict the energetic order of low-lying 3D , 3F , 1D , 1S , and 3P states. Experimentally, the ground state in the Pt atom is 3D_3 and the 3D_2 and 3F_4 substates are very close in energy to the ground state (the energy differences are only 776 ($^3D_3 - ^3D_2$) and 824 ($^3D_3 - ^3F_4$) cm^{-1} ; see Figure 3).

Separate MCSCF calculations for each state predict the ground state to be 3F , with the lowest 3D state lying at 1913 cm^{-1} above the 3F state without spin-orbit coupling. This may be the reason our prediction disagrees with the experimental results. Second-order CI (SOC) calculations have also been performed,²³ where the orbitals have been optimized for the lowest 3D state. Since the MCSCF orbitals have been optimized only for the 3D state, the 3F state is estimated to be relatively higher in energy; therefore, the energetic order of several low-lying electronic states is reasonable in comparison with that obtained by the MCSCF calculations (Figure 3).²⁴ The MCSCF+SOC/SBKJC(f) results suggest that a strong interaction occurs among the $J = 2$ substates; the lowest $J = 2$ state is obtained as a mixture of 1D_2 (51%) and 3D_2 (45%). Likewise, the second lowest $J = 2$ state consists of 3D_2 (43%), 1D_2 (24%), and 3F_2 (15%). The higher states behave in a similar manner.

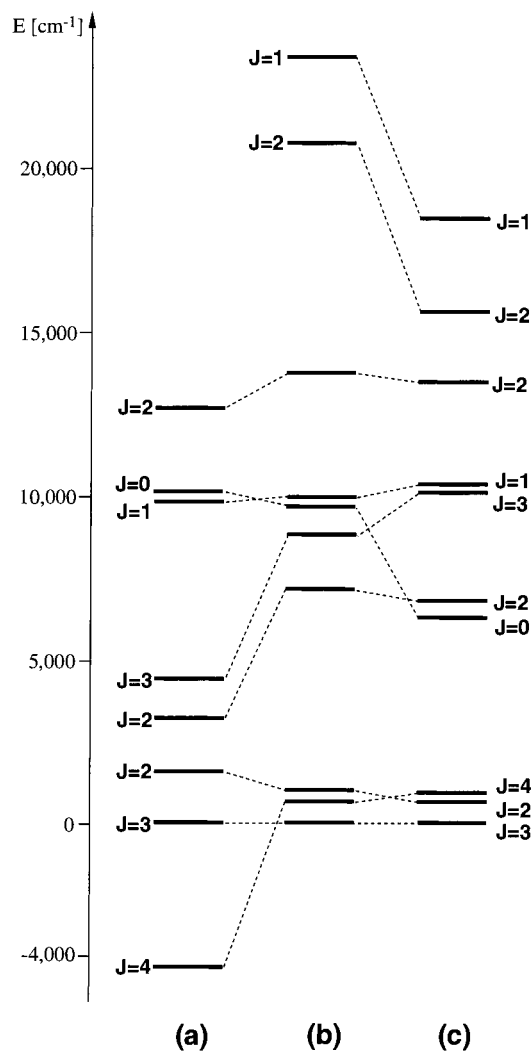


Figure 3. Spin-mixed states in atomic Pt: (a) MCSCF/SBKJC(f), (b) MCSCF+SOC/SBKJC(f), (c) experimental observation (ref 17).

Thus, 1D_2 strongly interacts with 3D_2 and 3F_2 . As a result, the lowest $J = 2$ state is considerably affected and the energy splitting between the lowest $J = 2$ and $J = 3$ states becomes very small ($\sim 50 \text{ cm}^{-1}$).

Similarly, the splitting energy between the lowest $^4P_{3/2}$ and $^4P_{1/2}$ in the Re atom is overestimated by 39%, even though the energy splitting between the $^4P_{5/2}$ and $^4P_{3/2}$ and between the lowest $^6D_{9/2}$ and $^6D_{7/2}$ is in good agreement with experimental results (errors of 8% and 3%, respectively). The MCSCF results without spin–orbit coupling show that the ground state is 6S and the lowest excited state is 6D ; the lowest 4P state is calculated to be higher in energy than the lowest 4G and 4D states. But, strong spin–orbit coupling makes $^4P_{5/2}$ the first excited state; this state has components of 33% $^4P_{5/2}$, 25% $^4D_{5/2}$, 15% $^4G_{5/2}$, and 14% $^2D_{5/2}$, so we have assigned this to $^4P_{5/2}$. $^4P_{3/2}$ and $^4P_{1/2}$ also have $^4D_{5/2}$ components of 37% and 31%, respectively. SOCI calculations lead to essentially the same results. Thus, there is strong spin–orbit interaction among the 4P , 4G , 4D , 6D , and other low-lying states. It therefore appears to be necessary to carry out extended MCSCF calculations with a larger active space, followed by very large spin–orbit CI calculations. Unfortunately, it is currently impractical to perform such calculations.

The Z_{eff} calculations do not reproduce the energy splittings of the lowest 5D state in Os and the lowest 4F state in Ir, though

TABLE 3: Energy Splittings [cm^{-1}] of the Lowest 5D State in Os^a

gap	exptl	MCSCF ^b	SOCI ^c
5D_4 – 5D_3	–4159.32	–4256.44	–3908.59
5D_3 – 5D_2	1418.83	–948.37	–894.69
5D_2 – 5D_1	–3025.65	–1574.56	–1464.72
5D_1 – 5D_0	–326.65	–638.65	–632.81
5F_5 – 5F_4	–3598.91	–3593.83	–3550.39
5F_4 – 5F_3	–2635.17	–2902.42	–2851.88
5F_3 – 5F_2	1212.02	–2183.80	–2179.80
5F_2 – 5F_1	–2854.09	–1549.02	–1389.71

^a Negative numbers indicate $E(^{2S+1}X_J) > E(^{2S+1}X_{J+1})$. ^b MCSCF/SBKJC(f). ^c MCSCF+SOC/SBKJC(f).

TABLE 4: Excitation Energy [cm^{-1}] of Low-Lying Spin States in Atomic Ir

gap	exptl	MCSCF ^a	SOCI ^b
$1^4F_{9/2}$	0.00	0.00	0.00
$2^4F_{9/2}$	2834.98	15182.24	6731.15
$1^4F_{3/2}$	4078.94	9071.82	8141.17 ^c
$1^4F_{5/2}$	5784.62	9679.79	9201.06
$1^4F_{7/2}$	6323.91	6831.39	6558.72
$2^4F_{7/2}$	7106.61	20702.94	11942.17
$2^4F_{5/2}$	9877.54	26001.17	16500.70
$2^4P_{3/2}$	10578.68	13502.40	12789.39 ^c
$2^4F_{3/2}$	11831.09	27700.77	17426.12
$2^4P_{1/2}$	12505.68	17973.52	16366.93

^a MCSCF/SBKJC(f). ^b MCSCF+SOC/SBKJC(f). ^c According to our calculated results, the lower state mainly has a $^2P_{3/2}$ component, while $1^4F_{3/2}$ is the main configuration in the higher state.

the energy splittings between the lowest and the next lowest substates are close to the experimental ones.¹⁷

In atomic Os, spectroscopic observation indicates that the $J = 2$ substate is lower in energy than the $J = 3$ substate of the lowest 5D , 5F , and 3F states (Table 3). The energy difference between 5D_3 and 5D_2 is calculated to be one-fourth that between 5D_3 and 5D_4 , but 5D_3 is still lower in energy than 5D_2 in our calculations. The MCSCF results show that 5D_3 and 5D_4 interact weakly with other states, while 5D_2 , 5D_1 , and 5D_0 have 3P components of 10~20%. Accordingly, it can be said that our estimation of spin–orbit interactions for the latter three states is not adequate to describe the correct energetic order of these spin-mixed states. We have found that dynamic correlation effects tend to decrease the energy difference between the 5D_3 and 5D_2 states²³ but still do not give even qualitative agreement for their energetic order.

In atomic Ir, two low-lying 4F states are calculated to be very close in energy without spin–orbit coupling (the energy difference between two $^4F_{9/2}$ substates is about 1000 cm^{-1}). Accordingly, quite strong spin–orbit interaction could occur between the substates of these electronic states. In fact, the experiments¹⁷ exhibit a strange energetic order of $J = 9/2, 3/2, 5/2, 7/2$ in the lowest 4F state, while the second lowest 4F has “normal” irregular ordering of $J = 9/2, 7/2, 5/2, 3/2$. The MCSCF energetic ordering of spin states (Table 4) is quite different from the experimental one. The MCSCF results indicate that there is strong interaction between the lowest $^4F_{3/2}$ and $^2P_{3/2}$; the lowest $J = 3/2$ state consists of 34% $^2P_{3/2}$, 33% $^4F_{3/2}$, and 23% $^2D_{3/2}$, which may be assigned as $^2P_{3/2}$. The second $J = 3/2$ state has 46% $^4F_{3/2}$, 28% $^2P_{3/2}$, and 24% $^4P_{3/2}$ so that this would be assigned as $^4F_{3/2}$. If the lowest $J = 3/2$ state is assigned not to $^2P_{3/2}$ but to $^4F_{3/2}$, then when dynamic correlation is included via SOCI, the energetic order of the low-lying spin states is somewhat improved (Table 4), although the second $J = 7/2$ state is still too high in energy.

TABLE 5: Energy Splittings [cm⁻¹] of the Lowest ²D State in Cu, Ag, and Au

atom	state	exptl	MCSCF ^a	SOCI ^b
Cu	² S _{1/2}	0.000	0.00	0.00
	² D _{5/2}	11202.565	-4342.78	3898.71
	² D _{3/2}	13245.423	-2278.42	5940.35
	ΔE ^c	2042.858	2064.36	2041.64
Ag	² S _{1/2}	0.00	0.00	0.00
	² D _{5/2}	30242.26	25029.82	26746.55
	² D _{3/2}	34714.16	29511.02	31191.69
	ΔE ^c	4471.90	4481.20	4445.14
Au	² S _{1/2}	0.0	0.00	0.00
	² D _{5/2}	9161.3	4850.84	6321.61
	² D _{3/2}	21435.3	16964.29	18359.07
	ΔE ^c	12274.0	12113.45	12037.46

^a MCSCF/SBKJC(f). ^b MCSCF+SOCI/SBKJC(f). ^c ΔE = E(²D_{3/2}) - E(²D_{5/2}).

TABLE 6: Spin–Orbit Splittings in the Lowest ³P States of Zn, Cd, and Hg

	Zn	Cd	Hg
Z _{eff}	330	1584	9040
state	³ P ₀ – ³ P ₁	³ P ₁ – ³ P ₂	³ P ₀ – ³ P ₁
calculated	162.03	491.59	459.69
exptl	190.08	388.93	542.11
error [%]	15	26	15

Thus, when some electronic states are close to each other in energy and strong spin–orbit interactions exist among their substates, our MCSCF and MCSCF+SOCI predictions often become unreliable, even qualitatively, as described in this section. Extended MCSCF or MCSCF+CI calculations should be performed for such complicated electronic states. In addition, more sophisticated investigation beyond the one-electron approximation may be needed in order to describe such strongly coupled states. Such situations may occur less frequently in molecular systems.

3.3. Coinage and Closed-Shell Metals (Groups 11 and 12).

The observed ground state of Cu is ²S, but the MCSCF energy of ²S (3d¹⁰4s¹) is higher in energy than that of ²D (3d⁹4s²) obtained with separate MCSCF calculations for each state, even though our prediction is reasonable for the splitting of the ²D state (see Table 5). We recalculated the excitation energies and the spin–orbit splittings of the ²D states in the Group 11 elements (Cu, Ag, and Au) at the MCSCF+SOCI level of calculation.²³ The excitation energy is still underestimated in Cu (Table 5), but the energetic order of states is correct at this computational level. On the other hand, the spin–orbit splittings are not affected very much by the improvement of wave functions and our predictions remain reasonable. The spin–orbit splittings in the lowest ²P states of these atoms are rather underestimated. The reason for this might be the fact that this state has a closed d subshell (5d¹⁰6p¹), as discussed below.

Zn, Cd, and Hg could be classified as main group elements, rather than transition metal elements, since they have closed d subshells in their ground states. If one employs the main group scale factors

$$f_4 = 11, \quad f_5 = 33, \quad f_6 = 113$$

for the fourth, fifth, and sixth rows of the periodic table, the predicted spin–orbit splittings for the lowest ³P states in Zn, Cd, and Hg are obtained as listed in Table 6, where the factors for semicore basis sets are selected^{10b} since *n*sp and *nd* orbitals are included in this ECP basis sets as well as (*n* + 1)sp orbitals. The errors in these calculated splittings are dramatically reduced

to less than 30%, supporting the notion that these elements should be treated as main group elements.

Summary

The one-electron Z_{eff} method for predicting spin–orbit splittings has been successfully used for many low-lying electronic states of the first- through third-row transition metal elements, with errors on the order of 30% or less. The consecutive third row elements Re, Os, Ir, and Pt have larger errors, which were discussed in some detail, and suggestions for possible error sources were proposed. It is clear that use of the Z_{eff} approach for transition metals is more problematic than in main group elements. In large part, this is due to the complications arising from the many low-lying states, leading to greater interactions among levels with the same *J* values. In some cases, it is necessary to include additional states arising from other terms or configurations to get more accurate results. Similar behavior has been observed in recent work on lanthanide ions²⁵ where it is found necessary to include the interaction with all states close in energy to the lowest levels in the spin–orbit Hamiltonian. It is important to add that the large numbers of interacting states will also cause difficulties for all-electron calculations, requiring large active spaces and large multi-reference CI wave functions for that level of theory as well.

The Z_{eff} values determined in this study are applicable only when d orbitals are important active orbitals in the description of electronic states. Expanding the MCSCF active space to include Rydberg orbitals is expected to provide improved spin–orbit splittings for higher electronic states of both transition metal and main group elements. Of course, such an expanded active space will result in very large MCSCF active spaces for molecular systems; such MCSCF calculations can become very demanding. Since the Z_{eff} approach may not be very reliable for the heaviest transition elements, we are now performing full Breit–Pauli calculations on the third-row transition metals and will compare them with these Z_{eff} results.²⁶ Then, subsequent papers will report the relativistic potential energy curves for molecules; we are now very interested in those of some transition metal hydrides and oxides.

Acknowledgment. Financial support from a grant-in-aid for Scientific Research (08640645 and 09554035) from the Ministry in Education, Science and Culture, Japan (to S.K.) and the DOD CHSSI software development program (to M.S.G.) is gratefully acknowledged.

References and Notes

- (1) Richards, W. G.; Trivedi, H. P.; Cooper, D. L. *Spin-orbit coupling in molecules*; Clarendon Press: Oxford, 1981.
- (2) (a) King, H. F.; Furlani, T. R. *J. Comput. Chem.* **1988**, *9*, 771. (b) Furlani, T. R.; King, H. F. *J. Chem. Phys.* **1985**, *82*, 5577.
- (3) Pyykkö, P. *Chem. Rev.* **1988**, *88*, 563.
- (4) Yarkony, D. R. *Modern Electronic Structure Theory*; World Scientific: Hong Kong, 1995; Parts 1 and 2.
- (5) Balasubramanian, K. *Relativistic Effects in Chemistry*; John Wiley and Sons: New York, 1997; Parts A and B.
- (6) Walker, T. E. H.; Richards, W. G. *J. Chem. Phys.* **1970**, *52*, 1311.
- (7) Cohen, J. S.; Wadt, W. R.; Hay, P. J. *J. Chem. Phys.* **1971**, *71*, 2955.
- (8) (a) Hay, P. J.; Wadt, W. R.; Kahn, L. R.; Raffanetti, R. C.; Phillips, D. H. *J. Chem. Phys.* **1979**, *71*, 1767. (b) Wadt, W. R. *Chem. Phys. Lett.* **1982**, *89*, 245.
- (9) Langhoff, S. R. *J. Chem. Phys.* **1980**, *73*, 2379.
- (10) (a) Koseki, S.; Schmidt, M. W.; Gordon, M. S. *J. Phys. Chem.* **1992**, *96*, 10768. (b) Koseki, S.; Gordon, M. S.; Schmidt, M. W.; Matsunaga, N. *J. Phys. Chem.* **1995**, *99*, 12764. (c) Koseki, S. Unpublished results for the sixth-row typical elements: Z_{eff}(Cs) = 12 210, Z_{eff}(Ba) = 12 432, Z_{eff}(Tl) = 9153, Z_{eff}(Pb) = 18 204, Z_{eff}(Bi) = 18 426, Z_{eff}(Po) = 18 648, Z_{eff}(At) = 18 870.

- (11) Matsunaga, N.; Koseki, S.; Gordon, M. S. *J. Chem. Phys.* **1996**, *104*, 7988.
- (12) (a) Stevens, W. J.; Basch, H.; Krauss, M. *J. Chem. Phys.* **1984**, *81*, 6026–6033. (b) Stevens, W. J.; Basch, H.; Krauss, M.; Jasien, P. *Can. J. Chem.* **1992**, *70*, 612–630. (c) Cundari, T. R.; Stevens, W. J. *J. Chem. Phys.* **1993**, *98*, 5555–5565.
- (13) (a) Ehlers, A. W.; Boehme, M.; Dapprich, S.; Gobbi, A.; Hoellwarth, A.; Jonas, V.; Koehler, K. F.; Stegmann, R.; Veldkamp, A.; Frenking, G. *Chem. Phys. Lett.* **1993**, *208*, 111–114. (b) Hoellwarth, A.; Boehme, M.; Dapprich, S.; Ehlers, A. W.; Gobbi, A.; Jonas, V.; Koehler, K. F.; Stegmann, R.; Veldkamp, A.; Frenking, G. *Chem. Phys. Lett.* **1993**, *208*, 237–240.
- (14) (a) Ruedenberg, K.; Schmidt, M. W.; Dombek, M. M.; Elbert, S. T. *Chem. Phys.* **1982**, *71*, 41–49, 51–64, 65–78. (b) Schmidt, M. W.; Gordon, M. S. *Annu. Rev. Phys. Chem.* **1998**, *49*, 233–266.
- (15) Schmidt, M. W.; Baldrige, K. K.; Boatz, J. A.; Elbert, S. T.; Gordon, M. S.; Jensen, J. H.; Koseki, S.; Matsunaga, N.; Nguyen, K. A.; Su, S.; Windus, T. L.; Dupuis, M.; Montgomery, J. A., Jr. *J. Comput. Chem.* **1993**, *14*, 1347–1363.
- (16) Huber, K. P.; Herzberg, G. *Constants of Diatomic Molecules*; Van Nostrand Reinhold: New York, 1979.
- (17) Moore, C. E. Atomic Energy Levels. *Nat. Stand. Ref. Data Ser.* **1949, 1952, 1958**, 35, V.I–III.
- (18) Stevens, W. J.; Krauss, M. *Chem. Phys. Lett.* **1982**, *86*, 320.
- (19) Heinemann, C.; Schwarz, J.; Koch, W.; Schwarz, H. *J. Chem. Phys.* **1995**, *103*, 4551, and private communication.
- (20) Solomonik, V. Private communication.
- (21) Schmidt, M. W. Unpublished results.
- (22) Heinemann, C.; Koch, W.; Schwarz, H. *Chem. Phys. Lett.* **1995**, *245*, 509.
- (23) Second-order CI calculation (MCSCF+SOC), where only a set of nd orbitals and $(n + 1)s$ orbital are MCSCF active and the external space of SOC calculation includes $(n + 1)p$ orbitals and one additional set of sp and d orbitals. The orbitals added are the lowest eigenvectors of the standard MCSCF Fock operator.
- (24) Heinemann et al. obtained the correct energetic order of the lowest 3F and 3D states using MCSCF wave functions with SBKJC(2f) basis set (f exponents used are 0.2 and 0.08).
- (25) Sanoyama, E.; Kobayashi, H.; Yabushita, S. *J. Mol. Struct. (THEOCHEM)*, submitted to special issue in honor of Prof. Shigeru Huzinaga.
- (26) Koseki, S.; Fedorov, D.; Schmidt, M. W.; Gordon, M. S. In preparation.